Reduced light-scattering properties for mixtures off spherical particles: a simple approximation derived from Mie calculations

Graaff, R.; Aarnoudse, J.G.; Zijp, J.R.; Sloot, P.M.A.; de Mul, F.F.M.; Greve, J.

DOI
10.1364/AO.31.001370

Publication date
1992

Published in
Applied Optics

Reduced light-scattering properties for mixtures of spherical particles: a simple approximation derived from Mie calculations

R. Graaff, J. G. Aarnoudse, J. R. Zijp, P. M. A. Sloot, F. F. M. de Mul, J. Greve, and M. H. Koelink

The reduced scattering cross section per unit of volume $\Sigma_s' \equiv \Sigma_s(1 - g)$ is an important parameter to describe light propagation in media with scattering and absorption. Mie calculations of the asymmetry factor g for nonabsorbing spheres and Q_{sca}, the ratio of the scattering cross section Σ_s and the particle cross section, show that $Q_{sca}(1 - g) = 3.28x^{0.37}(m - 1)^{2.09}$ is true to within a few percent, when the Mie parameters for relative refractive index m and size x are in the ranges of $1 < m \leq 1.1$ and $5 < x < 50$, respectively. A ratio of reduced scattering cross sections for radiation at two wavelengths is also independent of the size within the range mentioned, even for mixtures of different size spheres. The results seem promising for biomedical applications.

Key words: Mie scattering, multiple scattering, medicine, biology, light propagation in blood and tissue.

Introduction

Simulations of light scattering in media with scattering and partly absorbing particles such as spheres, and also such as red blood cells and scatterers in living tissues, can be performed by using Monte Carlo simulations[1–3] or the transport theory.[4–9] The basic properties of the scatterers, such as σ_a and σ_s, the absorption and scattering cross sections, and g, the asymmetry factor, which is the average cosine of the scattering angle, must be available. A reduced scattering cross section $\sigma_s' \equiv \sigma_s(1 - g)$ for a single scatterer can be defined.

In the diffusion approximation of transport theory, light propagation within a scattering medium with a given geometry can be fully described by Σ_a and $\Sigma_s' \equiv \Sigma_s(1 - g)$, where Σ_a and Σ_s are the absorption and scattering cross sections per unit volume. However, the validity of the diffusion approximation of the transport equation is restricted to cases in which the reduced albedo $c' \equiv \Sigma_s'/(\Sigma_a + \Sigma_s')$ is close to 1.[7]

Previous studies, using rigorous solutions of the transport equation for Henyey–Greenstein scattering[10] as well as for Rayleigh–Gans scattering,[8,9] have confirmed the validity of the diffusion approximation for values of c' close to 1.0. A more important conclusion from these studies was that light propagation in the whole range of $0 < c' < 1$ proved to be almost insensitive to changes in g when the values of σ_a and σ_s' are unchanged and g remains in the range between 0.9 and 1. It has been concluded therefore that σ_a and σ_s' are the properties that mainly influence light propagation within scattering media where $g \geq 0.9$. Scatterers within that range of g include red blood cells and the main part of scatterers within the human skin.[11]

The aim of this study is to investigate the Mie results for the property σ_s' for single spherical particles without absorption as a function of size and relative refractive index. Results are compared with data reported by others. The applicability of the results to spheres with small values of the absorption cross section and to mixtures of spheres of different sizes is discussed. It is assumed throughout that the

R. Graaff and J. G. Aarnoudse are with the Center for Biomedical Technology and Department of Obstetrics and Gynecology, University of Groningen, Oostersingel 59, Groningen 9713 EZ, The Netherlands. J. R. Zijp is with the Laboratory for Materia Technica, University of Groningen, Ant. Deusinglaan 1, Groningen 9713 AV, The Netherlands. P. M. A. Sloot is with the Department of Computer Systems, University of Amsterdam, Kruislaan 409, Amsterdam 1098 SJ, The Netherlands. F.F.M. de Mul, J. Greve, and M.H. Koelink are with the Department of Applied Physics, University of Twente, P.O. Box 217, Enschede 7500 AE, The Netherlands.

Received 1 December 1989.
0003-6935/92/101370-07$05.00/0.

scattering process at a single particle is not influenced by other particles. Possible application of the present results to the scattering properties of blood and tissues (e.g., the skin) is also discussed.

Mie Scattering for a Single Sphere

Methods

Values of σ_s' can be derived for single spherical particles that are illuminated by a plane wave by using Mie theory.[10,12] The scattered field is determined by the size parameter $x = 2\pi a/\lambda$, where a and λ represent the particle radius and the wavelength in the surrounding medium of the particle, and by m, the ratio of the refractive indices of particle and surrounding medium. Absorption by the spherical particle can be considered as well in Mie theory but is not taken into account in this study.

It is well known that the solution of equations for Mie scattering can lead to serious numerical problems, including decreased accuracy and instability, especially when recurrence relations for the Riccati–Bessel functions are not chosen with care.[13,14] Therefore, tabulated results of Mie calculations of different origins are compared in this study.

Our results have been obtained with Mie scattering calculations performed by Zijp, using upward recurrence, and by Sloot, using downward recurrence. Zijp used a program based on the equations given by van de Hulst,[10] running on a personal computer with a coprocessor. The program of Sloot *et al.*[15] is a modified version of the homogeneous sphere program reported by Bohren and Huffman,[16] running on a Cyber 205 computer.

Values of $\sigma_s' \equiv \sigma_s(1 - g)$ can be determined from $Q_{sca} \equiv \sigma_s/\pi a^2$, a dimensionless representation of the scattering cross section, and g (Ref. 13):

$$Q_{sca} = \frac{2}{x^2}\sum_{n=1}^{N}(2n+1)(|a_n|^2 + |b_n|^2), \quad (1)$$

$$g = \frac{4}{x^2 Q_{sca}}\sum_{n=1}^{N}\left[\frac{n(n+2)}{n+1}\mathrm{Re}(a_n a_{n+1}^* + b_n b_{n+1}^*) + \frac{2n+1}{n(n+1)}\mathrm{Re}(a_n b_n^*)\right], \quad (2)$$

where a_n and b_n are complex Mie coefficients and the * denotes complex conjugation. The programs of Sloot and Zijp both calculate Q_{sca} from Eq. (1). Values for g from Eq. (2) are provided only by the program of Zijp. However, it is also possible to determine σ_s and g from the sum of the angular intensity functions $i_1(\theta)$ and $i_2(\theta)$[10]:

$$Q_{sca} = \frac{1}{x^2}\int_0^{\pi}[i_1(\theta) + i_2(\theta)]\sin(\theta)d\theta, \quad (3)$$

$$g = \frac{\int_0^{\pi}[i_1(\theta) + i_2(\theta)]\cos(\theta)\sin(\theta)d\theta}{\int_0^{\pi}[i_1(\theta) + i_2(\theta)]\sin(\theta)d\theta}. \quad (4)$$

Equations (3) and (4) were applied to the tabulated values of $i_1(\theta) + i_2(\theta)$, which were calculated for each degree from the scattering functions $S_1(\theta)$ and $S_2(\theta)$ (see Ref. 10, p. 125) by the programs of Sloot and Zijp. In this way possible differences caused by the different recurrence relations could be detected. The Simpson rule was used for the numerical integrations.

Angular Intensity Functions

The angular intensity functions $i_1(\theta)$ and $i_2(\theta)$ are functions of x and m. Distributions for the same values of x and m have been compared in order to validate our results. Results for $x = 35$ and $m = 1.2$ are shown in Table I. The values of Ashley and Cobb,[17] who used the data of Gumprecht and Sliepcevich,[18] deviate from the other values for many angles, whereas our results with the programs of Zijp and Sloot are in agreement with each other.

Scattering Cross Sections and Asymmetry Factors

Values for g and Q_{sca} have been obtained by using Eqs. (1) and (2) with the program of Zijp for values of x up to 50 and for m between 1.025 and 1.20. The results are shown in Figs. 1 and 2. The results show the well-known major oscillations of the values of Q_{sca} and g for increasing values of the size parameter.[10,12,19] The major oscillations in Q_{sca} can be described for $m \approx 1$ with the anomalous diffraction theory as a function of $2x(m - 1)$.[10] Minor oscillations, or ripples, are found when $m > 1.1$ and $x > 15$.[12,19]

Data in the ranges of $x \leq 50$ and $1.025 \leq m \leq 1.20$ are shown in Tables II and III. The values for Q_{sca} as calculated from Eq. (1) by both programs deviate by

Table I. Angular Intensity Functions for x = 35 and m = 1.2 for a Spherical Particle as Calculated by Several Mie Programs

	$\frac{i_1(\theta) + i_2(\theta)}{2}$		
		This Work	
$\frac{180}{\pi}\theta$ (degrees)	Ashley and Cobb[17]	Sloot *et al.*[15]	Zijp[10]
0	341000	341035	341036
10	6995	7873	7873
20	4612	4245	4245
30	1201	1189	1189
40	388.5	393.1	393.0
50	159.8	173.6	173.6
60	106.1	108.5	108.5
70	76.27	76.26	76.26
80	42.34	39.56	39.55
90	3.46	3.46	3.46
100	13.99	13.99	13.99
110	42.59	29.99	29.99
120	97.38	94.21	94.20
130	70.02	70.05	70.04
140	112.2	112.4	112.3
150	92.76	86.83	86.83
160	590.2	135.7	135.7
170	284.9	278.7	278.7
180	1478	1478	1478

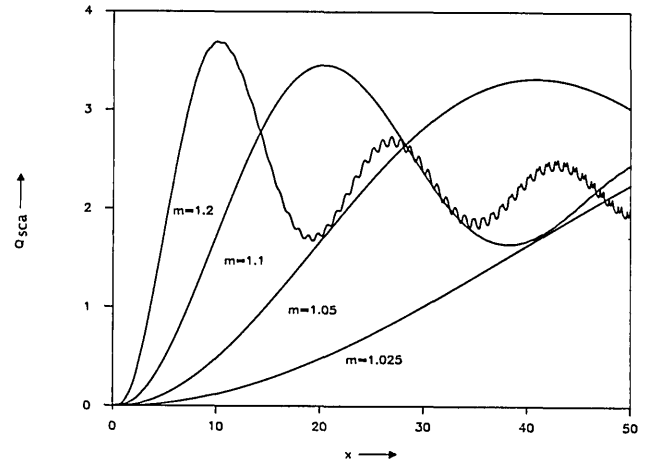

Fig. 1. Q_{sca} for Mie scattering of nonabsorbing spheres as a function of size parameter x and relative refractive index m.

<0.0003% from each other. The numerical inaccuracy of our results with Eq. (1) is therefore probably small, since both Sloot, using a Cyber computer, and Zijp, using a different program on a different computer, predict the same values for Q_{sca} for all the values listed in Table II, even in the range of minor oscillations. Values of g, as calculated by using Eq. (4) from the tabulated angular intensity functions of both programs, deviate by <0.0001% from each other.

Larger differences are found between the values for Q_{sca} obtained by using Eqs. (1) and (3). However, these differences are smaller than 0.24% for the whole range of m and x given in Table II. The differences are introduced by the 1° step size for numerical integration, which may be unacceptable for accurate results, especially for the larger values of x where fast changes in the angular intensity functions occur. Similar differences are found between values for g obtained by using Eqs. (2) and (4), which remain smaller than 0.026% in the whole range of m

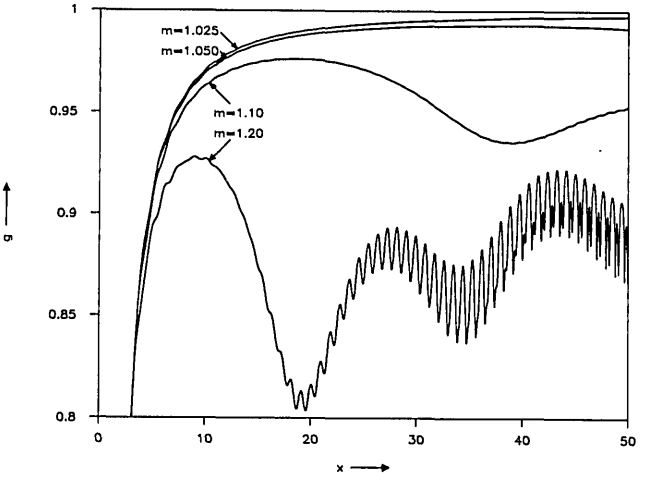

Fig. 2. Average cosine of the scatter angle g for Mie scattering of nonabsorbing spheres as a function of size parameter x and relative refractive index m.

Table II. Q_{sca} from Mie Calculations with Eq. (1) as a Function of x and m

x	m = 1.025	m = 1.05	m = 1.10	m = 1.20
5	0.02909	0.11822	0.47705	1.76997
10	0.12283	0.48353	1.71399	3.68513
15	0.27565	1.02865	2.92471	2.48889
20	0.48094	1.66478	3.44678	1.73269
25	0.73015	2.29275	3.12835	2.58556
30	1.01313	2.81916	2.36398	2.36019
35	1.31845	3.17298	1.75595	1.89957
40	1.63396	3.31666	1.67479	2.31762
45	1.94734	3.25098	2.03799	2.31562
50	2.24667	3.01270	2.44616	1.98649

and x listed in Table III. The values calculated by using Eqs. (1) and (2) are therefore preferred.

The values of Q_{sca} and g of Chu *et al.*,[20] as given by van de Hulst[5] for m = 1.2 and x = 5–25, agree with the current results for both Q_{sca} and g as shown in Table IV. The data for Q_{sca} of Wickramasinghe[21] for x = 5–15 and m = 1.1 and 1.2 also agree with our results. However, the data for g as given by Wickramasinghe are probably in error, since they deviate seriously from the data of Chu *et al.*[20] and the data presented here.

Reduced Scattering Cross Sections of a Sphere

The results for the product $Q_{sca}(1 - g)$ are given in Fig. 3 and Table V. It is remarkable that the major oscillations, which are present in Q_{sca} as well as in g, do not appear in this product. This might be related to the fact that $Q_{sca}(1 - g)$ also equals the change in efficiency for radiation pressure, Q_{pr}, for nonabsorbing particles after scattering:

$$Q_{pr} \equiv Q_{abs} + Q_{sca}(1 - g). \quad (5)$$

Some fluctuations occur for $x < 5$, which seem to be independent of m. However, the minor oscillations, or ripples, in Q_{sca} and g, which are found when $m > 1.1$ and $x > 15$ and depend on m, do not disappear in $Q_{sca}(1 - g)$.[12,19] These minor oscillations in $Q_{sca}(1 - g)$ may be related to resonant behavior of surface waves.[10] For larger values of x or m, the amplitude of the ripple structure becomes larger and more complex.[19]

Ashkin and Dziedzic[22] were able to determine experimentally the ripple structure of the efficiency factor

Table III. g from Mie Calculations with Eq. (2) as a Function of x and m

x	m = 1.025	m = 1.05	m = 1.10	m = 1.20
5	0.908486	0.908254	0.906288	0.893395
10	0.971047	0.969707	0.963360	0.927325
15	0.985079	0.983240	0.974602	0.874356
20	0.990546	0.988519	0.975931	0.815940
25	0.993320	0.991046	0.971115	0.866150
30	0.994932	0.992245	0.959126	0.888786
35	0.995928	0.992746	0.941815	0.851400
40	0.996580	0.992763	0.935953	0.879317
45	0.997034	0.992315	0.945343	0.920582
50	0.997356	0.991412	0.953363	0.873612

Table IV. Q_{sca} and g from Mie Calculations Compared with the Results of Chu *et al.* and Wickramasinghe for Different Values of x with $m = 1.2$

	Chu *et al.*[20]		Wickramasinghe[21]		This Work	
x	Q_{sca}	g	Q_{sca}	g	Q_{sca}	g
5	1.770	0.893	1.7700	0.7958	1.7700	0.8934
10	3.685	0.927	3.6851	0.9073	3.6851	0.9273
15	2.489	0.874	2.4889	0.8729	2.4889	0.8744
20	1.733	0.816	—	—	1.7327	0.8159
25	2.586	0.866	—	—	2.5856	0.8662

for radiation pressure. They applied optical levitation to single oil drops and showed excellent agreement between the changes of the intensity needed for levitation and the ripple structure in Q_{pr} that is predicted by Mie theory.

Approximations

Reduced Scattering Cross Sections

It is possible to fit a large part of the data for $Q_{sca}(1 - g)$ in the range where the influence of the ripple can be neglected:

$$[Q_{sca}(1 - g)]_{pred} = 3.28x^{0.37}(m - 1)^{2.09}, \quad (6)$$

as shown in Fig. 3. The given coefficients have been derived by trial and error for values of x and m in the range where $g > 0.90$: $5 < x < 50$ and $1 < m \leq 1.1$. This is the range for scattering in blood and a large part of scatterers within living tissues. The inaccuracy introduced by Eq. (6) is restricted to a few percent. With the aid of Table V different values for the coefficients may be chosen if only a part of the present range has to be described with higher accuracy. Table VI gives the ratio between the predicted values and the results of Mie calculations. Equation (6) shows that $Q_{sca}(1 - g)$ can be split into a refractive-index-dependent factor and a size-dependent factor, as in the Rayleigh–Debye–Gans equations for intensity at a distance r from a sphere with radius a,

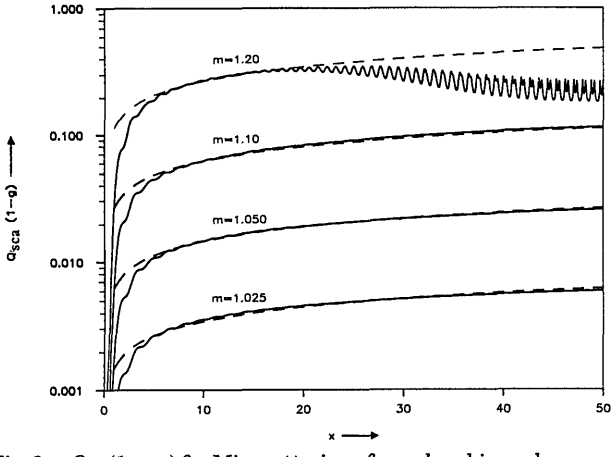

Fig. 3. $Q_{sca}(1 - g)$ for Mie scattering of nonabsorbing spheres as a function of size parameter x and relative refractive index m. The dashed curves represent the predictions of Eq. (6).

Table V. $Q_{sca}(1 - g)$ from Mie Calculations with Eqs. (1) and (2) as Functions of x and m

x	$m = 1.025$	$m = 1.05$	$m = 1.10$	$m = 1.20$
5	0.002662	0.010846	0.044705	0.18869
10	0.003556	0.014648	0.062800	0.26782
15	0.004113	0.017240	0.074282	0.31271
20	0.004547	0.019113	0.082959	0.31892
25	0.004877	0.020529	0.090364	0.34608
30	0.005135	0.021863	0.096624	0.26249
35	0.005369	0.023017	0.102170	0.28228
40	0.005589	0.024002	0.107264	0.27970
45	0.005776	0.024983	0.111390	0.18390
50	0.005940	0.025874	0.114081	0.25107

illuminated by an intensity I_0 (Refs. 10 and 12):

$$I(\theta) = \frac{I_0}{2} x^4 \frac{a^2}{r^2} \left|\frac{m^2 - 1}{m^2 + 2}\right|^2 \times \left\{\frac{3}{u^3}[\sin(u) - u\cos(u)]\right\}^2 [1 + \cos^2(\theta)], \quad (7)$$

with

$$u = 2x \sin(\theta/2). \quad (8)$$

In the Rayleigh–Gans approximation, g is independent of m and Q_{sca} is proportional to $[(m^2 - 1)/(m^2 + 2)]^2$ or $(m - 1)^2$ if $m \approx 1$. As a consequence, $Q_{sca}(1 - g)$ will be proportional to $(m - 1)^2$. However, in our range of application, $(m - 1)^{2.09}$ best describes the refractive-index-dependent term of the Mie results.

The results for Mie calculations have been compared with Rayleigh–Gans calculations, as shown in Fig. 4. Therefore, Eq. (7) was rewritten in the following form[10]:

$$i_1(\theta) + i_2(\theta) = 2\frac{(2\pi r)^2}{\lambda^2}\frac{I(\theta)}{I_0} = x^6 \left|\frac{m^2 - 1}{m^2 + 2}\right|^2 \times \left\{\frac{3}{u^3}[\sin(u) - u\cos(u)]\right\}^2 [1 + \cos^2(\theta)]. \quad (9)$$

Q_{sca} and g are found by numerical integration with application of Eqs. (3) and (4) and Eq. (9) for 900

Table VI. $[Q_{sca}(1 - g)]_{pred}/[Q_{sca}(1 - g)]_{Mie}$ as a Function of x and m with $[Q_{sca}(1 - g)]_{pred} = 3.28x^{0.37}(m - 1)^{2.09}$

x	$m = 1.025$	$m = 1.05$	$m = 1.10$	$m = 1.20$
5	1.002	1.047	1.082	1.091
10	0.970	1.002	0.995	0.994
15	0.974	0.989	0.978	0.989
20	0.980	0.993	0.974	—
25	0.992	1.004	0.971	—
30	1.008	1.008	0.971	—
35	1.021	1.014	0.972	—
40	1.030	1.021	0.973	—
45	1.041	1.025	0.979	—
50	1.053	1.029	0.994	—

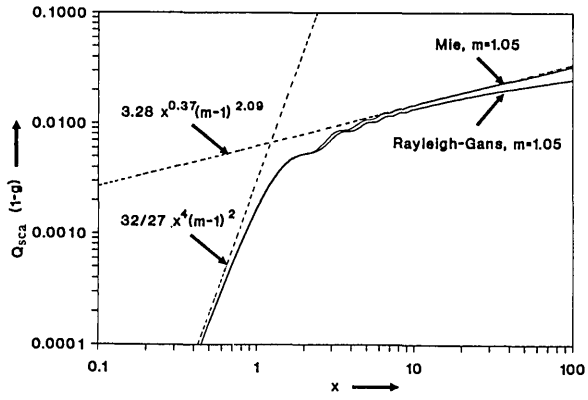

Fig. 4. Q_{sca} $(1 - g)$ for Rayleigh–Gans and Mie scattering ($m = 1.05$). Predictions according to Eq. (6) and Rayleigh scattering (assuming that $g = 0$) have been added.

angles. It appears that the Rayleigh–Gans theory predicts $Q_{sca}(1 - g)$ much better than Q_{sca} or g, since Q_{sca} is a factor of 4 too large for $x = 50$ and $m = 1.05$ with Rayleigh–Gans theory, whereas $Q_{sca}(1 - g)$ is only 20% too large. The behavior for $x < 5$ is depicted to advantage by the Rayleigh–Gans theory, as expected.

Another remarkable conclusion can be drawn from Eq. (6): the ratio of the reduced scattering cross sections at two different wavelengths is a function only of the wavelength ratio and the values of m. It can be further reduced to

$$\frac{\sigma_s'(\lambda_1)}{\sigma_s'(\lambda_2)} = \left(\frac{\lambda_2}{\lambda_1}\right)^{0.37}\left(\frac{m_1 - 1}{m_2 - 1}\right)^{2.09}. \tag{10}$$

The ratio of the reduced cross sections proves to be independent of the particle size in this range and can thus be predicted with an accuracy of a few percent without knowledge of the particle size. It is clear from Fig. 3 that such a relation cannot be derived in the range where rippling occurs.

Mixtures of Spheres

It is possible to calculate an average value of the reduced scattering cross section for a mixture of spheres, σ_s' (mixture), from individual values of $\sigma_{s,i}$ and g_i, if it is assumed that scattering at a single particle is not influenced by other particles and that angular intensities can be added without considering coherence. In this case we may write $I(\theta) = \Sigma\, \mathrm{frac}(i) I(\theta, i)$, where frac($i$) is the relative number of particles with angular intensity distribution $I(\theta, i)$. Substitution in Eqs. (3) and (4) shows that

$$\langle g \rangle = \frac{\langle x^2 Q_{sca} g \rangle}{\langle x^2 Q_{sca} \rangle} = \frac{\langle \sigma_s g \rangle}{\langle \sigma_s \rangle}, \tag{11}$$

where the fractions of the different scatterers should be weighted with their concentrations in the medium. For a mixture of scatterers, the following relation can then be derived:

$$\begin{aligned} \sigma_s'(\text{mixture}) &= \langle \sigma_s \rangle (1 - \langle g \rangle) \\ &= \langle \sigma_s \rangle - \langle \sigma_s g \rangle \\ &= \langle \sigma_s (1 - g) \rangle. \end{aligned} \tag{12}$$

The last term equals $\langle \sigma_s' \rangle$. This means that the reduced scattering cross section of a mixture σ_s' (mixture) can be derived from the individual values of $\sigma_s'(i)$ and their concentrations, without knowledge of the individual values of $\sigma_s'(i)$ and $g(i)$.

Substitution of Eq. (6) shows that it is even possible to apply Eq. (10) to mixtures of spheres when the size distribution, concentration, and refractive indices are unknown. However, $(m_1 - 1)/(m_2 - 1)$ must be available in that case and must have the same value for all spheres. And, of course, $m(i)$ and $x(i)$ must be within the range of validity of Eq. (10).

Influence of Absorption when $\sigma_a \ll \sigma_s$

When absorption is introduced with $\sigma_a \ll \sigma_s$, as in the case of red blood cells for 630 nm $< \lambda <$ 1000 nm, it has been shown by Mie calculations considering absorption that $\sigma_s + \sigma_a$ is approximately independent of absorption for red blood cells.[7] In that case σ_s can be found by subtraction of σ_a from the value found in Table II. Since it has also been recognized that values of g are virtually independent of small amounts of absorption,[7,12] it is possible to predict σ_s'. The validity of this correction method is supported by the figures of Irvine[19] for $m = 1.2$ and $x = 0$–30: it is possible to predict $\sigma_a + \sigma_s'$ to within 6% as long as $\tan(\beta) \equiv n'/(m - 1) \leq 0.10$. Herein, $n' = \gamma\lambda/(4\pi)$, where γ is the absorption coefficient of the material of the sphere, and values for σ_a are calculated with the relations given by Bohren and Nevitt.[23] However, this correction method cannot be used for mixtures where x and m are unknown.

When x and m are not known and Eq. (10) is to be used, another approach must be found. If $\sigma_a \ll \sigma_s$, we may neglect the influence of absorption on g and σ_s and thus on σ_s' and $Q_{sca}(1 - g)$. From the figures of Irvine for $m = 1.2$ and $x = 0$–30, it is found that the deviation of $\sigma_a + \sigma_s'$ from the Mie results without absorption is $<10\%$ as long as $n'/(m - 1) \leq 0.10$, and Q_{abs} is predicted with the anomalous diffraction approximation.[10] For many biomedical applications in which size distributions of particles are not known, this approximation is sufficient.

Biomedical Applications

In this section we discuss whether Eqs. (6) and (10) can be used to describe the scattering properties of red blood cells and several tissues. Relations such as Eqs. (6) and (10) might prove to be important for biomedical applications, especially in noninvasive applications in which light propagation is compared at several wavelengths, as in near-infrared spectroscopy and pulse oximetry. With these methods exact knowledge of phase functions and scattering coefficients is

not available because of the variation of these scattering properties between subjects and even with time, but with Eq. (10) it becomes possible to predict a ratio of reduced scattering coefficients.

Red blood cells are within the range of validity of Eq. (6) for size ($5 < x < 50$) and refractive index ($1 < m < 1.1$) for visible and infrared light. However, red blood cells are not spherically shaped, and the distance between adjacent red blood cells in blood vessels is short. Although Mie calculations are successful in predicting experimentally found values for σ_s of red blood cells,[7,24] they overpredict experimentally found values of σ_s' by a factor of up to 3 or more.[24] More work is therefore needed to overcome these discrepancies between theory and experiment in order to validate the use of Eq. (6) for nonspherical scatterers such as red blood cells. However, the influence of the nonspherical shape of scatterers and distance to adjacent scatterers on the *ratio* of reduced scattering cross sections is probably smaller than the influence of shape and distance on the scattering cross sections themselves. This may justify the use of Eq. (10) for red blood cells.

Differences between refractive indices within human tissues are probably small enough to obey $1.0 < m < 1.1$.[25] Measurements of the asymmetry factor with a goniometer by Flock *et al.*[26] at 633 nm for chicken and bovine muscle as well as pig brain were all above 0.94, indicating that the size of most scatterers within these tissues is large enough to fit in the $5 < x < 50$ range. Only a small fraction of the scatterers in these tissues might have a smaller size. However, much lower values ($0.6 < g < 0.8$) were found in tumor and adipose tissue.[26] For human dermis at 633 nm, the intensity distribution after single scattering, as measured by Jacques *et al.*,[27] indicates that 90% of the scattering events can be described with Henyey–Greenstein scattering with an asymmetry factor of 0.92. The remaining scattering events within the dermis samples have been ascribed to scattering by small scatterers.

For tissues with a relatively large amount of small scatterers, the following approach may be chosen. A similar description as with Eq. (10) can be used for the fraction of small scatterers, however, with the wavelength ratio to the power of 4.0 instead of 0.37, according to Rayleigh scattering, and 2.0 instead of 2.09 for the power of the refractive-index-dependent term[10]:

$$\frac{\sigma_{s,2}'(\lambda_1)}{\sigma_{s,2}'(\lambda_2)} = \left(\frac{\lambda_2}{\lambda_1}\right)^{4.0}\left(\frac{m_1 - 1}{m_2 - 1}\right)^{2.0}. \tag{13}$$

With knowledge of the fraction of σ_s' by small Rayleigh scatterers, f_2, at a given wavelength λ_0 and by applying the mixing rule as given by Eq. (12), we can derive

$$\frac{\sigma_s'(\lambda)}{\sigma_s'(\lambda_0)} = \frac{\sigma_{s,1}'(\lambda)}{\sigma_{s,1}'(\lambda_0)}[1 - f_2(\lambda_0)] + \frac{\sigma_{s,2}'(\lambda)}{\sigma_{s,2}'(\lambda_0)} f_2(\lambda_0), \tag{14}$$

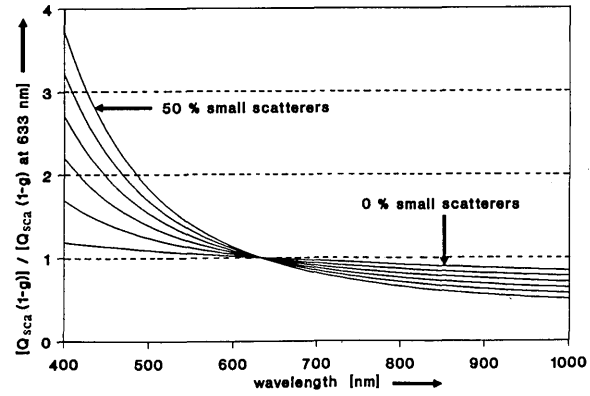

Fig. 5. Wavelength dependence of $Q_{sca}(1 - g)$ for mixtures of scatterers in the range of validity of Eq. (10) and various fractions of contributions by Rayleigh scatterers at 633 nm (0%, 10%, 20%, 30%, 40%, and 50%).

where the first term is given by Eq. (10) and the second term by Eq. (13). Figure 5 shows the results for $f_2(\lambda_0) = 0 - 0.5$, with $\lambda_0 = 633$ nm and assuming no wavelength dependence on m. The contribution of small scatterers increases rapidly for lower wavelengths and decreases rapidly for higher wavelengths. Therefore, from the human dermis data of Jacques *et al.*[27] with $f_2(633) = 0.1$, we can expect that Eq. (10) can also be applied with reasonable accuracy to human dermis within the range of red and near-infrared light.

Conclusions

The reduced scattering cross section is an important parameter for the description of light propagation in scattering media. This reduced scattering cross section can be predicted to within a few percent for spherical particles in the ranges of $5 < x < 50$ and $m \leq 1.10$ with the simple equation given [Eq. (6)]. Larger deviations have been observed as soon as the ripple is observed: for $m > 1.1$ when $x \geq 15$. Corrections for small amounts of absorption can be made.

However, it is more important that the ratio of reduced scattering cross sections at different wavelengths can be predicted for a medium with spherical particles without a precisely known size distribution and refractive index as long as x and m are within the range of validity of our equation and scattering at a single particle is not influenced by other particles. The ratio $(m_1 - 1)/(m_2 - 1)$ has to be known. In these conditions, Eq. (10) can be applied to biomedical multiwavelength applications such as whole blood oximetry, pulse oximetry, and tissue spectroscopy.

References

1. R. A. J. Groenhuis, H. A. Ferwerda, and J. J. Ten Bosch, "Scattering and absorption of turbid materials determined from reflection measurements. 1: Theory," Appl. Opt. **22**, 2456–2462 (1983).
2. H. W. Jentink, F. F. M. de Mul, R. G. A. M. Hermsen, R. Graaff, and J. Greve, "Monte Carlo simulations of laser Doppler blood

flow measurements in tissue," Appl. Opt. **29,** 2371–2381 (1990).
3. H. W. Jentink, F. F. M. de Mul, R. Graaff, H. E. Suichies, J. G. Aarnoudse, and J. Greve, "Laser Doppler flowmetry: measurements in a layered perfusion model and Monte Carlo simulations of measurements," Appl. Opt. **30,** 2592–2597 (1991).
4. K. M. Case and P. F. Zweifel, *Linear Transport Theory* (Addison-Wesley, Reading, Mass., 1967).
5. H. C. van de Hulst, *Multiple Light Scattering* (Academic, New York, 1980), Vols. 1 and 2.
6. P. S. Mudgett and L. W. Richards, "Multiple scattering calculations for technology II," J. Colloid Interface Sci. **39,** 551–567 (1972).
7. L. Reynolds, C. Johnson, and A. Ishimaru, "Diffuse reflectance from a finite blood medium: applications to the modeling of fiber optic catheters," Appl. Opt. **15,** 2059–2067 (1976).
8. R. Graaff, J. G. Aarnoudse, F. F. M. de Mul, and H. W. Jentink, "Light propagation parameters for anisotropically scattering media, based on a rigorous solution of the transport equation," Appl. Opt. **28,** 2273–2279 (1989).
9. R. Graaff, J. G. Aarnoudse, F. F. M. de Mul, and H. W. Jentink, "Improved expressions for anisotropic scattering in absorbing media," in *Scattering and Diffraction,* H. A. Ferwerda, ed., Proc. Soc. Photo-Opt. Instrum. Eng. **1029,** 103–110 (1989).
10. H. C. van de Hulst, *Light Scattering by Small Particles* (Wiley, New York, 1957).
11. M. J. C. Van Gemert, S. L. Jacques, H. J. C. M. Sterenborg, and W. M. Star, "Skin optics," IEEE Trans. Biomed. Eng. **36,** 1146–1154 (1989).
12. M. Kerker, *The Scattering of Light and Other Electromagnetic Radiation* (Academic, New York, 1969).
13. W. J. Wiscombe, "Improved Mie scattering algorithms," Appl. Opt. **19,** 1505–1509 (1980).
14. W. A. de Rooij and C. C. A. H. van der Stap, "Expansion of Mie scattering matrices in generalized spherical functions," Astron. Astrophys. **131,** 237–248 (1984).
15. P. M. A. Sloot, A. G. Hoekstra, H. van der Liet, and C. G. Figdor, "Scattering matrix elements of biological particles measured in a flow-through system: theory and practice, Appl. Opt. **28,** 1752–1762 (1989).
16. C. F. Bohren and D. R. Huffman, *Absorption and Scattering of Light by Small Particles* (Wiley, New York, 1983).
17. L. E. Ashley and C. M. Cobb, "Single particle scattering functions for latex spheres in water," J. Opt. Soc. Am. **48,** 261–268 (1958).
18. R. O. Gumprecht and C. M. Sliepcevich, *Tables of Light Scattering Functions for Spherical Particles* (U. Michigan Press, Ann Arbor, Mich., 1951).
19. W. M. Irvine, "Light scattering by spherical particles: radiation pressure, asymmetry factor, and extinction cross section," J. Opt. Soc. Am. **55,** 16–21 (1965).
20. C. M. Chu, G. C. Clark, and S. W. Churchill, *Tables of Angular Distribution Coefficients for Light Scattering by Spheres* (U. Michigan Press, Engineering Research Institute Publication, Ann Arbor, Mich., 1957).
21. N. C. Wickramasinghe, *Light Scattering Functions for Small Particles* (Hilger, London, 1973).
22. A. Ashkin and J. M. Dziedzic, "Observation of optical resonances of dielectric spheres by light scattering," Appl. Opt. **20,** 1803–1814 (1981).
23. C. F. Bohren and T. J. Nevitt, "Absorption by a sphere: a simple approximation," Appl. Opt. **22,** 774–775 (1983).
24. J. M. Steinke and A. P. Shepherd, "Comparison of Mie theory and the light scattering of red blood cells," Appl. Opt. **27,** 4027–4033 (1988).
25. F. P. Bolin, L. E. Preuss, R. C. Taylor, and R. J. Ference, "Refractive index of some mammalian tissues using a fiber optic cladding method," Appl. Opt. **28,** 2297–2303 (1989).
26. S. T. Flock, B. C. Wilson, and M. S. Patterson, "Total attenuation coefficient and scattering phase functions of tissues and phantom materials at 633 nm," Med. Phys. **14,** 835–841 (1987).
27. S. L. Jacques, C. A. Alter, and S. A. Prahl, "Angular dependence of helium–neon laser light scattering by human dermis," Lasers Life Sci. **1,** 309–333 (1987).